Title: Tensile and hydraulic properties of geosynthetics after mechanical damage and abrasion laboratory tests.

Authors: A. Rosete[1], P. Mendonça Lopes[2], M. Pinho-Lopes[*3] and M.L. Lopes[4]

[1] Ph.D. student, Department of Civil Engineering, University of Aveiro, and Research Fellow, Department of Civil Engineering, Faculty of Engineering, University of Porto, Campus Universitario de Santiago, 3810-193 Aveiro, Portugal, Telephone: +351 234 370 049, Fax: +351 370 094, E-mail: anarosete@ua.pt or anarosete@fe.up.pt

[2] Research Fellow, Department of Civil Engineering, University of Aveiro, Campus Universitario de Santiago, 3810-193 Aveiro, Portugal, Telephone: +351 234 370 049, Fax: +351 370 094, E-mail: pmlopes@ua.pt

[3] Assistant Professor, Department of Civil Engineering, University of Aveiro, Campus Universitario de Santiago, 3810-193 Aveiro, Portugal, Telephone: +351 234 370 049 extension 24613, Fax: +351 370 094, E-mail: mlopes@ua.pt

[4] Full Professor, Department of Civil Engineering, Faculty of Engineering, University of Porto, Rua Dr. Roberto Frias, s/n 4200-465 Porto Portugal, Telephone: +3515081564; Fax: +3515081446; E-mail: lcosta@fe.up.pt

[*] Corresponding author

Abstract:

Installation damage of geosynthetics occurs during their handling, positioning on the ground and placing and compacting of fill material. Abrasion is a common damage mechanism where there is cyclic relative motion (friction) between a geosynthetic and contact soil. This paper presents the laboratory test results of mechanical damage and abrasion performed on six geosynthetics. The in isolation and combined effects on mechanical, hydraulic and physical properties of the geosynthetics were assessed. Results show that the effects of induced mechanical and abrasion damage essentially depend on the geosynthetic structure. For the most affected materials, strength losses after abrasion (in isolation and combined with mechanical damage) are higher than after the induced mechanical damage. Therefore, for most geosynthetics studied, abrasion is the conditioning mechanism which most affects their tensile strength. An increase of the characteristic opening size of the geosynthetics was observed, while their permittivity did not increase. This may be caused by differences in the test setups.

Keywords:
Geosynthetics, mechanical damage, abrasion, tensile strength, permittivity, characteristic opening size, laboratory tests

1 INTRODUCTION

Installation damage of geosynthetics can significantly affect their performance and results from their handling and placing, and from the compaction actions associated with the placement of fill material. Traditionally, installation damage has been assessed mainly for reinforcement applications of geosynthetics, focusing on changes in their tensile properties. For applications where other functional properties are required corresponding assessments should also be done, for example for hydraulic properties.

Two types of abrasion are mentioned in the literature: 1) a consequence of installation damage, induced by the placement and compaction of the fill material (reported by Bräu (1998) and Allen and Bathurst (1994)); 2) time-dependent abrasion during the materials' service lifetime (Shukla 2002). This paper refers to the second type of abrasion, which results from cyclic relative motion (friction) between the geosynthetic and contact soil during service, which is particularly important for geosynthetics in railway applications, temporary roads, canal revetments, sea shores with sediments and sliding masses washing up and down (Watn and Chew 2002).

This work aims at contributing to understanding the effect of mechanical damage and abrasion (in isolation and combined, sequentially) on the mechanical and hydraulic properties of six geosynthetics, using laboratory tests. To assess the influence of mechanical and abrasion damage, tensile and hydraulic tests (where relevant) were performed, accompanied by visual inspections. The characteristic opening size of the materials was also determined. From the tensile tests results the influence of the nominal strength, the type of the geosynthetic, the maximum loading used in the mechanical damage test and the type of induced damage mechanism are discussed. Besides strength losses, strain and stiffness reductions were analysed. The changes in normal permeability and the characteristic opening size are discussed and compared. From the results, reduction factors are determined and synergetic effects are assessed by comparing the reduction factors obtained for their combined effect with the factors obtained by the traditional approach (multiplication of separate reduction factors).

2 BACKGROUND

The durability of geosynthetics can be grouped into factors related to their endurance and degradation (Koerner 2005). This paper focus on two endurance durability factors: mechanical damage (associated with installation) and abrasion. While the first usually leads to immediate changes in a geosynthetic's properties, the second is time-dependent. Their combined effect, although little studied, can be relevant to several applications of geosynthetics.

There are a number of published studies on installation damage of geosynthetics, especially for reinforcement applications. They show the degree of mechanical damage resulting from installation depends on (Watn and Chew 2002): characteristics of the geosynthetic; the grain size, the angularity and the thickness of the fill material; the procedures and the construction equipment; the climatic conditions. More recently Hufenus et al. (2005) concluded the survivability of a geosynthetic depends primarily on the type of fabric structure and secondarily on the nature of the polymer.

In the design of geosynthetics, installation damage is usually represented by a reduction factor (RF_{ID}) representing the associated tensile strength losses. For reinforcement applications, additional strength losses due to creep and degradation due to chemical and biological processes are usually considered in the design. The corresponding reduction factors are multiplied, assuming there is no synergy between them. There are some proposals in the literature for estimating the installation damage reduction factor as the matrix to assess the survivability of geosynthetics after installation by Hufenus et al. (2005). However, the value of the reduction factor for installation damage (RF_{ID}) is usually determined using field installation damage tests where the reinforcement installation method, the type of backfill and the compaction method are the same as or similar to the project conditions using a common test protocol (Bathurst et al. 2011). If installation damage data for specific conditions are not available, interpolations can be taken from existing measurements with different soils for the same geosynthetics, or interpolations considering other products within the same product line (PD ISO/TR 20432:2007). Traditionally, the design of geosynthetics uses a safety factor approach. Recently Bathurst et al. (2011) have presented a reliability-based analysis and load and resistance factor design calibration using data from installation damage tests, computing installation damage bias statistics for six different categories of geosynthetic and four categories of backfill soils, classified according to the average soil particle size (D_{50}).

Installation damage also results in abrasion effects, local decrease of material thickness, fibre cutting, puncturing, and in the worst case complete disintegration along a

given area of geosynthetic (Bräu 1998). Installation damage is usually associated with loss of resistance, however, Allen and Bathurst (1994) suggest using a residual stiffness modulus to more adequately measure the resistance to site installation damage for woven polyester geogrids and polyethylene geogrids, rather than using peak strength retained after damage (which can be conservative).

Although field tests should be the primary source of information on installation damage (as in Lim and McCartney (2013), Bathurst et al. (2011), Hufenus et al. (2005), Bräu (1998), Allen and Bathurst (1996)), several authors have used laboratory tests for simulating it. For example, Huang (2006), Huang and Chiou (2006) and Huang and Wang (2007) studied flexible geogrids, assessing index properties (tensile strength, strain or stiffness). Huang and Wang (2007) mention that the standard laboratory test, ENV ISO 10722-1, can be modified to properly simulate field installation damage by using an aggregate similar to that used in the field and changing the cyclic load intensity.

For non-reinforcement applications of geosynthetics the actions resulting from the installation processes can be significantly higher than the tensile or normal contact stresses which these materials are subjected to during their lifetime, or to the corresponding stresses considered in their design (Shukla 2002). Therefore, to ensure the material's survivability they have to be adequately accounted for. Additionally, it is likely that installation damage affects functional properties of the geosynthetics, other than tensile properties. For example, for separation and/or filtration, Christopher and Elias (1998) mention that the holes resulting from installation damage may change the characteristic opening size of the geosynthetics, and therefore their hydraulic properties. Watn and Chew (2002) point out that abrasion resulting from installation damage can reduce the thickness of the geosynthetic and hence lead to a local reduction of its strength and change its filtration and separation properties. However, such changes in relevant properties need to be adequately quantified. Rosete et al. (2012) gave an initial contribution by performing mechanical damage laboratory tests on different (reinforcement and drainage) geocomposites to assess their effects on mechanical or hydraulic properties. The results showed considerable strength losses for reinforcement geocomposites. For drainage geocomposites the results suggest that besides the cuts, clogging of geotextile pores may occur during installation of geosynthetics.

Abrasion is another important durability factor for geosynthetics, although less studied. It is particularly important for geosynthetics in applications where during service there can be wearing of their surfaces as a result of rubbing the geosynthetic against a surface (Shukla 2002). Some studies have been done, in particular on the abrasion of geosynthetics

used in railway structures. Van Dine et al. (1982) first reported an assessment of abrasion processes and their severity on samples of woven and non-woven geotextiles with mass per unit area between 137 g/m^2 and 730 g/m^2. The most frequent abrasion processes on woven geotextiles were peeling, splitting and cutting, while on non-woven geotextiles they were peeling, flattening, clumping and cutting. The studies of Hausmann et al. (1990) on abrasion of geotextiles in railway tracks concluded that the loss of tensile strength seems to be related to the mass per unit area of the material and the volume of traffic. Perforations in the geotextiles were detected, which didn't compromise the separation function. Huang and Liao (2007) used a cylindrical chamber to study the abrasion damage of geogrids used to manufacture geosynthetic containers. They distinguish abrasion damage in turbid flow, associated with 'in-service' conditions, and 'installation damage' which occurs during compaction stages of earthwork projects. Equations to facilitate the assessment of abrasion damage proposed by Huang et al. (2007) can be useful in linking in-field abrasion damage of a tested geotextile to that obtained in laboratory index tests (sliding block sand paper method).

For some applications geosynthetics have to adequately withstand both installation damage and abrasion, maintaining minimum values of relevant functional properties. Lopes and Pinho-Lopes (2010) reported a laboratory study on the combined effect of mechanical and abrasion damage in two non-woven spun-bounded geotextiles with different mass per unit areas using laboratory tests. In the mechanical damage laboratory tests (adapted from ENV ISO 10722-1) the aggregate used was ballast. Due to the characteristics of the ballast particles the effects of mechanical damage were quite severe, resulting in cuts and perforations. The synergetic effect (positive or negative) between mechanical and abrasion damage was different for the two geotextiles studied. This paper aims to contribute to understanding endurance durability by analysing the combined effect of mechanical damage (associated with installation processes) and abrasion on mechanical, hydraulic and physical properties of six geosynthetics using laboratory tests.

3 GEOSYNTHETICS

The materials studied were: two nonwoven geotextiles consisting of continuous mechanically bonded polypropylene (PP) filaments (GTX1 and GTX2); two geogrids, a PP extruded biaxial geogrid (GGRe) and a woven geogrid composed of high modulus polyester (PET) fibres knitted in a flat orientation and covered with a protective polymeric coating (GGRw); two uniaxial geocomposites (GCR1 and GCR2) composed of high modulus PET fibres attached to a nonwoven continuous filament geotextile backing.

Table 1 includes nominal values of some of the geosynthetics' properties, namely: the peak tensile strength (T_{nom}) and strain at break (ε_{nom}) at machine direction, the permittivity (ψ_{nom}), the characteristic opening size ($O_{90\ nom}$), the mass per unit area (mua_{nom}) of the products containing a geotextile, the thickness (t_{nom}); and the grid spacing of the geogrids (equal for machine and cross machine direction). The GGRe junctions have a nominal thickness of 5.8 mm while the longitudinal and transversal ribs have a nominal thickness of 2.2 and 1.4 mm, respectively.

4 LABORATORY TESTS

4.1 Test program

The test program consisted of performing laboratory tests on geosynthetic samples to simulate mechanical damage under cyclic loading, abrasion damage and the effect of abrasion damage on samples previously subjected to the mechanical damage laboratory test (combined effect). To characterise the undamaged and damaged samples different laboratory tests were used: wide-width tensile tests (EN ISO 10319:2008), tests to assess water permeability characteristics normal to the plane, without load (EN ISO 11058:2010) and tests to determine the characteristic opening size (EN ISO 12956:2010).

Tables 2 and 3 summarise the test program implemented. The procedures used to induce mechanical damage and abrasion damage in the laboratory are briefly described in the following section. For reasons of time and material availability the hydraulic properties were assessed only for GTX2 and GCR1.

4.2 Mechanical and abrasion damage

The laboratory simulation of mechanical damage under cyclic loading of the geosynthetics followed the method described in EN ISO 10722:2007, in which a synthetic aggregate of sintered aluminium oxide (corundum) is used. The test method was setup in laboratory to simulate the installation damage of geosynthetics (ENV ISO 10722-1:1998). In this study, besides the maximum cyclic loading of 500 kPa (from EN ISO 10722:2007) tests using a maximum cyclic loading of 900 kPa were also performed, according to ENV ISO 10722-1:1998.

For abrasion damage simulation the procedures described in EN ISO 13427:1998 were used. The test consists of placing a geosynthetic specimen on the upper plate of a stationary platform where it is rubbed by a P100 abrasive. The abrasive is placed on the lower plate and

196 moved along a horizontal axis under controlled pressure. To effectively simulate the abrasion
197 on the geosynthetics studied it was necessary to adjust the procedures, namely changing the
198 position of the materials on the plates. Because of the stiffness of GGRe, the specimen was
199 placed on the lower plate and the abrasive on the upper plate. For GTX1 and GTX2 it was
200 necessary to place a P24 abrasive film between the specimen and the upper plate to ensure
201 that during the test the specimen did not adhere to the abrasive film placed on the lower plate.
202 This caused no additional damage to the geotextile specimens.

203 **4.3 Characterisation of the geosynthetics**

204 The characterisation of the geosynthetics included visual inspections of the different
205 types of samples (undamaged and damaged), to better understand the impact and the severity
206 of the induced damage. The visual inspections were done with the naked eye and were
207 registered with photographs, using rulers as a scale reference.

208 To determinate the water permeability characteristics normal to the plane without load
209 the constant head method described in EN ISO 11058:2010 was followed. The test consists of
210 subjecting a single unloaded layer of geotextile or a related product to a unidirectional flow of
211 water normal to the plane under five values of constant head losses (70, 56, 42, 28 and 14
212 mm). The tests allowed estimating the flow velocity value at a temperature of 20ºC
213 corresponding to a head loss of 50 mm (VI_{H50}, mm/s). The permittivity (ψ, s^{-1}) was obtained
214 by dividing VI_{H50} by the head loss of 50 mm. In each test five specimens were used.

215 The determination of the characteristic opening size of the geosynthetics followed the
216 procedures of EN ISO 12956:2010. In these tests a granular material was washed through a
217 specimen used as a sieve (wet sieving) without load, under specific conditions. The particle
218 size distribution curve of the granular material passing the sample was determined. The
219 characteristic opening size of each specimen (O_{90}, µm) is equal to the d_{90} of the particle size
220 distribution curve, where d_{90} is the particle size for which 90% of the mass fraction is smaller
221 than the mass of measured particles. In each test three specimens were used.

222 The tensile tests were carried out using the procedures described in EN ISO
223 10319:2008 and the strains were measured with a video-extensometer. Different jaws were
224 used (compressive block jaws for the extruded geogrid, capstan for the woven geogrid and
225 wedge jaws for the geotextiles and reinforcement geocomposites) in order to avoid slippage
226 in the clamping area. To characterize each sample five specimens were tested, according to
227 EN ISO 10319:2008.

5 RESULTS AND DISCUSSION

5.1 Visual inspection

The visual observation of undamaged and damaged specimens allowed comparing their structures and the corresponding changes induced. With the naked eye the effects induced by the mechanical damage tests using a maximum loading of either 500 kPa or 900 kPa are identical, although the effects of the damage induced with a higher loading were more pronounced. Table 4 lists the visual changes observed in the geosynthetics after the laboratory damage tests and Figures 1 to 4 illustrate some of those effects.

Visually, the extruded geogrid (GGRe) was the material least affected by mechanical and abrasion damage induced in the laboratory tests, although abrasion (either in isolation or combined with mechanical damage) induced reductions of about 13% of its junctions. In the abrasion tests on GGRe only its junctions were in contact with the abrasive (Figure 1) as its junctions are thicker (5.8 mm) than its ribs (1.4 mm and 2.2 mm, respectively, for the transversal and longitudinal ribs).

After mechanical damage of the woven geogrid (GGRw) some fibber cutting and incrustation of fine particles was found (Figure 2-a). These fine particles resulted from the fragmentation of corundum during the test. However, the most severe effects were observed after the abrasion damage tests of both undamaged and previously mechanically damaged specimens (Figure 2-b and 2-c). The abrasion caused detachment of the protective polymeric coating, and disaggregation, cuts and splitting of some transversal and longitudinal ribs.

The visually observed changes for the geotextiles (GTX1 and GTX2) and the geocomposites (GCR1 and GCR2) were the incrustation of fines after mechanical damage and detachment and cuts of some PET yarns (for the geocomposites). The changes observed on these geosynthetics after abrasion and after mechanical damage followed by abrasion (Figures 3 and 4, Table 4) are in good agreement with those reported by Van Dine et al. (1982).

Apparently the combined effect of mechanical damage and abrasion is quite severe for the geocomposites studied. The damage observed in the PET yarns (which provide most of the strength) was particularly severe, as they were cut and detached from the geotextile backing and suffered superficial disaggregation.

The visual appearance of the geotextile and geocomposite samples subjected to mechanical damage followed by abrasion is quite similar (Figures 3-c and 4-c). It seems that the effects of previously induced mechanical damage enabled the detachment and superficial disaggregation of filaments, which gave rise to the perpendicular accumulation of fibres in the machine direction of these geosynthetics.

5.2 Results of laboratory tests

Table 5 summarises the mean values of permittivity (ψ, s^{-1}) and the characteristic opening size (O_{90}, µm) of GTX2 and GCR1. Table 6 includes a summary of the mean results of tensile tests: maximum tensile strength (T_{max}, kN/m), strain at break (ε_f, %) and secant tensile stiffness modulus at 2% of strain ($J_{sec\ 2\%}$, kN/m). The mean results (Table 5 and 6), similar to Hufenus et al. (2005), are presented with 95% confidence intervals and were estimated assuming the results can be approximated by normal distribution functions. According to relevant standards, all results refer to five (valid) specimens, except the characteristic opening size which refers to 3 specimens.

From the test results the residual values of the relevant properties were determined using Equation 1, where R_Y is the residual value (in %) after damage of the property considered (Y), Y_{dam} is the mean value of Y for the damaged sample and Y_{und} is the corresponding mean value for the undamaged sample.

$$R_Y = \frac{Y_{dam}}{Y_{und}} \quad (1)$$

Reduction factors (RF) for mechanical damage, abrasion damage and the cumulative effect of mechanical damage followed by abrasion were determined (Equation 2) from the test results. To assess if there is synergy between the damage mechanisms considered, the last was compared with the traditional reduction factor, obtained by multiplying the reduction factors determined for each damage mechanism, acting in isolation and considered as independent. Reduction factors for tensile strength, permittivity and characteristic opening size were determined. These factors can be used for comparative purposes but should not be used for design, as they result from laboratory simulations.

$$RF = \frac{1}{R_Y} \quad (2)$$

5.3 Effects on the permittivity and on the characteristic opening size

Figure 5 represents the relationships obtained from the hydraulic tests between head loss and flow velocity at 20ºC for GTX2 and GCR1 before and after laboratory damage tests. The data and the fitted quadratic regression curve plotted (according to EN ISO 11058:2010) correspond to the specimen nearest to the mean curve for the corresponding sample.

Figure 5 shows that, as expected, the flow velocity at 20ºC increases with the increasing of head loss. For both GTX2 (Figure 5-a) and GCR1 (Figure 5-b) the curves of undamaged samples and after mechanical damage and after isolated abrasion damage are very close to each other, compared to the curve for the combination of the two types of damage. The combination of mechanical and abrasion damage reduced the permittivity of these geosynthetics.

From Table 5, after abrasion the permittivity of GTX2 and GCR1 remained practically unchanged (0.6% reduction and increase, respectively), while the characteristic opening size (O_{90}) increased about 25% for GTX2 and decreased 1.6% for GCR1. After mechanical damage the permittivity of GCR1 remained unchanged, when compared with the undamaged sample, and O_{90} increased about 45%. For GTX2 the permittivity decreased 13%, although its O_{90} increased about 32% after the induced mechanical damage. After the combination of mechanical and abrasion damage the permittivity of GTX1 and GCR1 decreased about 30% and 16%, respectively, while for the O_{90} values there was an increase which was more significant for GTX2 (about 33%) than for GCR1 (about 7%). For most samples, for the same geosynthetic and quantity, the 95% confidence interval is similar. However, for the characteristic opening size obtained after mechanical and abrasion damage combined, such an interval is high, particularly for GCR1. This is a result of two factors: the number of tested specimens is small (3); and the scattering of results is more important.

Visual inspection after mechanical damage tests essentially showed the incrustation of fine particles resulting from corundum fragmentation. Therefore, it would be expected that the permittivity and the characteristic opening size of the geosynthetics would decrease because of the prior clogging of some of its pores. Before the tests the specimens were not cleaned, however, according to relevant standards, they were submerged in water for 12 hours, which may have contributed to releasing some of the clogging particles. To determine the characteristic opening size the specimens were submitted to a water flow of 0.5 l/min under a pressure of about 300 kPa, which may also have caused some of the particles to go through the specimen during the test. Therefore, it is likely that the apparently contradictory results are only a consequence of the different test procedures used.

In terms of permittivity for these geosynthetics, the cumulative effect of induced mechanical and abrasion damage is more severe than estimated from the traditional approach (Table 7). These conclusions, if confirmed for real conditions, indicate that where relevant the combined effect of these damage mechanisms should be considered, other than their superposition.

The reduction factors for the characteristic opening size have to be carefully analysed because an increase of the characteristic opening size of the geosynthetics after damage is likely (resulting in RF<1.0). Nevertheless, for coherence, Equation 2 was used. For the characteristic opening size an opposite trend was found, as the cumulative effect of mechanical and abrasion damage is less severe to these geosynthetics than estimated from the traditional approach (Table 8).

5.4 Effects on the tensile properties

5.4.1 General

The effect of the damage induced on the tensile properties of the geosynthetics studied is clear from Table 6. To better understand the results obtained, the influence on some parameters is assessed and discussed.

5.4.2 Influence of nominal tensile strength

To evaluate the influence of the nominal tensile strength on the damage induced in terms of the residual values of tensile strength, peak strain, and stiffness for 2% of strain, two groups of geosynthetics were considered with similar structures but different nominal strength values:

1. Geotextiles, GTX1 and GTX2, with 50 kN/m and 55 kN/m, respectively (Figure 6);
2. Reinforcement geocomposites, GCR1 and GCR2, with 55 kN/m and 75 kN/m, respectively (Figure 7).

In terms of nominal strength, the differences between the geotextiles are not too significant, as GTX2 has a nominal strength only 10% higher than GTX1. Although having a similar structure, GTX1 thickness and mass per unit area are 20% and 25% lower, respectively, than GTX2, therefore it would be expected that the residual strength values for GTX1 after the induced laboratory damage would be lower. After mechanical damage with 900 kPa the residual tensile strength of GTX2 (83%) is slightly higher than that of GTX1 (80%). After mechanical damage with 900 kPa followed by abrasion the difference is more pronounced; 81% of residual strength for GTX2 and 72% for GTX1. After isolated abrasion the opposite occurs: the residual strength for GTX1 is higher than for GTX2 (96% and 85%, respectively). The residual strength values of the samples subjected to mechanical and abrasion damage (combined) are in agreement with the observed visual effects (Figure 3, Table 4) since they were more severe. In terms of tensile strength, the most conditioning damage mode for GTX1 seems to be mechanical damage, as the response of the specimens

submitted to mechanical damage followed by abrasion is nearer to that of the corresponding samples submitted only to mechanical damage. For GTX2 there is no evident trend: for mechanical damage with 900 kPa the trend is similar, while with 500 kPa the opposite occurred. The confidence intervals for the tensile strength after damage are relatively similar to those for undamaged samples (except after abrasion), indicating that the number of specimens used is acceptable. As far as the peak strain is concerned, for all the damage mechanisms considered the residual values of GTX2 are lower than those of GTX1. After isolated abrasion of GTX1 there was an increase of about 27% of the residual peak strain. The range of confidence limits for GTX1 peak strain is wider after damage, indicating a larger variability of this quantity. For GTX2 there is a mixed trend, while for some samples the confidence interval is narrower after damage, after abrasion and mechanical damage with 500 kPa (in isolation and combined) there is an increase of this interval relative to that for undamaged material. After the different types of induced damage the residual stiffness for 2% strain of GTX2 (between 79% and 114%) is always higher than for GTX1 (52% to 73%). After abrasion the stiffness for 2% of strain of GTX2 increases 14% relative to the undamaged material. For GTX1 the reductions of the stiffness for 2% of strain after mechanical and abrasion damage are higher than the tensile strength reductions. For GTX2, the opposite trend occurs after mechanical and isolated abrasion damage. Therefore, while for GTX1, for the conditions considered the results indicate that using the strength reductions instead of the stiffness for 2% of strain to characterise its behaviour would be conservative, for GTX2 the opposite occurs (except after the combined effect of mechanical and abrasion damage). The confidence intervals for the stiffness for 2% of strain (Table 6) are very wide (even for the undamaged material), indicating the corresponding results have to be used carefully and further confirmed by additional testing to obtain more statistically representative data.

For the geocomposites, the material with higher nominal strength (GCR2) has higher residual values of tensile strength for all the damage mechanisms simulated. Although the nominal strength of GCR2 is 36% higher, the residual tensile strength values of GCR2 after damage are not significantly higher than the ones for GCR1, with differences between 2% (after mechanical damage with 900 kPa and abrasion) and 18% (after mechanical damage with 900 kPa). For these materials abrasion is the most conditioning damage mechanism, particularly due to its effects on the PET yarns described previously (Figure 4, Table 4). The residual tensile strength values after abrasion and after mechanical damage followed by abrasion are quite similar and considerably lower than the ones obtained after isolated

mechanical damage. For the residual values of the peak strain there is no clear trend. After abrasion and after mechanical damage with 900 kPa the residual peak strain is larger for GCR2 (106% and 115%, respectively) than for GCR1 (48% and 95%); for the remaining damaged samples the opposite occurs. For the samples subjected to the combined effect of mechanical and abrasion damage the residual strains are between 75% and 80% for GCR1 and between 53% and 64% for GCR2, for maximum applied loadings of 500 kPa or 900 kPa, respectively. For all types of induced damage mechanisms, the residual stiffness values of GCR2 are higher than for GCR1. The stiffness for 2% of strain of GCR2 increased after the induced damage (residual value higher than 100%), except after isolated abrasion (reduction of 29%). The variability of the tensile strength, peak strain and stiffness can be important and in some cases is of the same order of magnitude as the corresponding mean value. Additional tests, increasing the number of specimens per type of sample, have to be done to confirm such trends. The tensile strength reductions of GCR1 and GCR2 after the considered damage mechanisms are conservative relative to the corresponding stiffness for 2% of strain. The safety margin is much more important for GCR2. The differences between the two materials (Table 1) also include the number of PET yarns (120 and 118 yarns per meter of width for GCR1 and GCR2, respectively), the mass per unit area (321 and 362 g/m^2, respectively) and the thickness (2.1 and 2.2 mm, respectively). Therefore, it is likely that GCR2 (stronger) would better endure the initial strains applied during the tensile tests.

5.4.3 Influence of the type of geosynthetic

The influence of the type of geosynthetic was assessed by comparing results for the GGRw woven geogrid, the GTX2 geotextile and the GCR1 reinforcement geocomposite, with a nominal strength of 55 kN/m and different structures (Table 6 and Figures 8 to 11).

For all the simulated damage mechanisms the residual tensile strength of GTX2 is the highest at over 80% (Figure 8). After abrasion, either in isolation or combined with mechanical damage, there is a significant reduction of the tensile strength of GGRw and GCR1. For these materials abrasion was clearly the most conditioning damage mechanism.

Although the fibres of GGRw are covered with a protective polymeric coating, this protection was removed (partially or totally) and the cuts and abrasion of the fibres (Figure 2) led to tensile strength reductions. As the connections between the longitudinal and transversal ribs of the geogrid are not integral, the material is sensitive to the effects of mechanical and abrasion damage. For GCR1, as the high modulus PET yarns are knitted to the geotextile backing, any cuts in the yarns or in their connections to the backing caused significant

decreases in tensile strength. GTX1 is manufactured using continuous filaments, which allows arching around damaged areas when subjected to loads during the tensile tests.

For each type of sample (composed by five valid specimens) a mean load-strain curve was obtained from the curves of those specimens. Such curves do not represent the real behaviour of the material, particularly after failure of one of the specimens. Therefore, for discussion purposes, the curve analysed for each type of sample was chosen as the curve for a particular specimen nearest to the corresponding mean curve. Figures 9 to 11, respectively, include such curves for GGRw, GTX2 and GCR1.

The load-strain curves of GGRw (Figure 9) undamaged and after mechanical damage with 500 kPa and 900 kPa are quite similar, despite the decrease in peak parameters (peak tensile strength and peak strain) after mechanical damage. The corresponding stiffness for 2% strain increased (17% and 13%) after mechanical damage (500 kPa and 900 kPa, respectively). After abrasion and after mechanical damage followed by abrasion there are significant reductions of the peak parameters of GGRw (Figure 8) and the gradient of the load-strain curves decreased significantly relative to the curve of the undamaged sample (reduction of stiffness for 2% of strain between 29% and 55%). Although the behaviour of the specimens in terms of peak values is quite similar their stiffness has some variability, which has to be taken into consideration. The abrasion damage affected the connections between perpendicular ribs, the coating and the fibres of GGRw more significantly than the mechanical damage did (Figure 2). The areas without coating were likely to have a more flexible response than those with coating, and the connections between ribs where there was relative movement as a consequence of damage were likely to limit the ability of the geogrid to transfer loads to adjacent areas during the tensile tests.

The load-strain curves of GTX2 (Figure 10) before and after the induced laboratory damage are similar. Particularly for lower strains, the load-strain curves after damage are very close, regardless of the type of damage mechanism considered. These curves represent the complete response of GTX2 measured in the tensile tests (until rupture). Nevertheless, for most applications it is likely that such strains are never achieved. The stiffness for 2% of strain (Table 6) increased after abrasion (about 14%) and decreased for all the other types of damaged samples (from 12% to 29%). The variability of the referred stiffness values (in some cases very important) should be noted. GTX2 is quite thick and heavy, so when superficial damage was induced by the laboratory tests the consequences were not very significant. Its homogeneous structure enabled the damage to be distributed along the surface of GTX2

without creating areas which were more affected than others. The changes observed influenced the mechanical response of GTX2, particularly for larger strains.

GCR1 (Figure 11) exhibits significant tensile strength, peak strain, and stiffness for 2% of strain reductions after the induced damage. This is in good agreement with the severe damage observed in the PET yarns and geotextile backing (Table 4). Similar overall behaviour was observed after mechanical damage (for both cyclic loadings considered) as for mechanical damage followed by abrasion (for both cyclic loadings). The stiffness for 2% of strain reductions after damage was important and ranged between 37% (mechanical damage with 500 kPa) and 73% (mechanical damage with both 500 kPa and 900 kPa followed by abrasion). The reductions observed for the peak strain were lower (varying between 20% and 52%); after mechanical damage with 900 kPa they were 5%. Abrasion largely affected the yarns of this geocomposite and also its base geotextile (similar to Figure 4b, for GCR2). As the yarns are largely responsible for the strength of GCR1 the reductions observed are to be expected. The mechanical damage, although less evident, also resulted in changes in the load-strain response of the material. The ability to withstand loads from the tensile tests was compromised by the induced damage.

The results show the structure of the geosynthetic has an influence on its response to the induced damage. GTX2 has a more uniform and continuous structure than GCR1, and GGRw was the material least affected by the laboratory damage tests performed.

5.4.4 Influence of the maximum loading in the mechanical damage tests

To evaluate the influence of the maximum loading used in the mechanical damage tests the residual strength of the GGRw woven geogrid, GTX2 geotextile, and GCR1 and GCR2 reinforcement geocomposites after mechanical damage with 500 kPa and 900 kPa were compared (Figure 12).

As expected, the residual strength was higher for the samples damaged with the lowest maximum loading (Figure 12). When the maximum loading was increased from 500 kPa to 900 kPa (approximately 45%); the differences found for the strength losses were not proportional. The corresponding variations of residual strength after mechanical damage with 500 kPa and 900 kPa are about 4% (GGRw), 9% (GTX2), 23% (GCR1) and 17% (GCR2).

In Figure 12 the residual tensile strength values after mechanical damage with 900 kPa versus 500 kPa are plotted. These refer to the older version of the corresponding test standard (ENV ISO 10722-1:1998, with 900 kPa) and the latest one (EN ISO 10722:2007, with 500 kPa). From Figure 12 it is clear which of the geosynthetics studied are the most sensitive

to induced mechanical damage - the reinforcement geocomposites GCR1 and GCR2. The equation relating these geosynthetics (of the same family of products) is also included for future reference.

5.4.5 Influence of the type of damage mechanism induced

Figure 13 summarises values of the residual tensile strength after laboratory damage tests (from Table 6) used to evaluate the influence of the type of damage mechanism of the geosynthetics studied. Figures 14-a and 14-b relate the residual tensile strength values after abrasion damage and after mechanical damage with 900 kPa and 500 kPa, respectively, followed by abrasion.

For most induced damage mechanisms the strength losses measured for GTX1 and GTX2 geotextiles and the extruded GGRe geogrid are much lower relative to the other geosynthetics. For GGRe the residual tensile strength after mechanical damage with 900 kPa is slightly above 100%. Pinho-Lopes et al. (2002) and Paula et al. (2004) reported similar results and suggested they can be related to some reorientation of the geogrid during the mechanical damage laboratory test. After abrasion damage and after mechanical damage followed by abrasion, although the GGRe nodes thickness decreased about 13%, the effects on the strength were not significant, 4% and 6% respectively (variability associated to the mean strength values on a similar order of magnitude). The connections between longitudinal and transversal ribs of GGRe are integral, and according to the results obtained it can be considered that the abrasion of the joints was only superficial and did not cause weakening of those connections.

The residual tensile strengths of the GTX1 and GTX2 geotextiles were also quite high. For GTX1, with lower mass per unit area and thickness, the residual tensile strength after abrasion damage and after mechanical damage with 900 kPa is about 96% and 80%, respectively. The effects of the previously induced mechanical damage could have made GTX1 more sensitive to the effect of abrasion induced later, as the residual tensile strength obtained is about 72%. For GTX2 there is no evident trend for a conditioning damage mechanism. Although apparently there were no significant changes after mechanical damage of the geotextiles (example in Figure 3a, for GTX2), it is likely that the fibre surfaces, in contact with the aggregate in the test, were affected (partial cuts). When later subjected to subsequent abrasion damage tests those cut fibres were rolled, undergoing reorientation and there was an accumulation of rolled fibres perpendicular to the direction of motion for the abrasion test (Figure 3c, for GTX2). The lower thickness and mass per unit area of GTX1

were likely to have enabled a more severe cumulative effect of mechanical and abrasion damage than for GTX2.

For GGRw, GCR1 and GCR2 the conditioning mechanism is abrasion damage, as their residual tensile strength after mechanical damage followed by abrasion is quite similar to the corresponding values obtained after abrasion damage acting in isolation. After mechanical damage the residual tensile strength values of GGRw, GCR1 and GCR2 are comparatively high. Such responses are related with the evident change of the materials' structure (Figures 1 and 4 and Table 4). Their structure, which includes connections between components that enable possible weaker points, increases their sensitivity to the induced abrasion. Further tests are needed (under real abrasion conditions) to clarify how realistic the mechanical response is after the laboratory abrasion damage tests. In the laboratory test, the area of abrasive in contact with the geosynthetic is quite significant. Under field conditions, for example, when the abrasion is caused by the movement of ballast in railway applications, this area is smaller (contact points between ballast and the geosynthetic) and depends on the compaction state of the aggregate and on their rearrangement associated with loading. In the field the severity of the abrasive action can be more important than in laboratory. The structure of these geosynthetics doesn't allow significant arching around damaged areas, which would spatially limit the effects of damage and strength reduction.

Figure 14 includes a line with 1:1 slope, representing points for which the induced mechanical damage has no influence on the residual tensile strength of the geosynthetics. The points corresponding to the test results are on or near that line, except for GTX1 (mechanical damage with 900 kPa). This confirms that abrasion is the most important induced damage mechanism. According to the positions of the points on the plots, it is clear that GGRw, GCR1 and GCR2 geosynthetics were those most affected by the induced in-laboratory damage since the corresponding points are relatively close to the origin in the graphs. For GTX1, mechanical damage is the most conditioning damage mechanism considered.

To assess a possible synergetic effect between the damage mechanisms considered, reduction factors for the tensile strength were determined (Table 9) using the data from the tests and the traditional approach. The minimum value for these reductions factors is 1.0. For GGRe (little affected by the damage induced) the resulting differences are insignificant (0.8%). For GTX1 the cumulative effect of mechanical and abrasion damage affects the tensile strength 6% more than expected from the traditional approach, indicating the traditional approach can be slightly unsafe. For the other materials and test conditions considered, the traditional approach leads to conservative results. For GGRw and GTX2 such

differences range between 24% and 14% (mechanical damage with 500 kPa) and 13% and 15% (mechanical damage with 900 kPa), respectively. As abrasion damage is the most conditioning mechanism, and when combined with it the effects of mechanical damage are very small, for GCR1 and GCR2 the traditional approach leads to very conservative results: 52% (for GCR2 after mechanical damage with 500 kPa) to 143% (for GCR1 after mechanical damage with 900 kPa) higher than the cumulative effects of mechanical and abrasion damage. If these conclusions are confirmed for real conditions the combined effects of mechanical and abrasion damage should be considered when relevant, rather than their superposition.

6 CONCLUSIONS

In this paper the behaviour of six different geosynthetics subjected to laboratory tests of mechanical and abrasion damage (in isolation and combined) was investigated. A visual inspection of the samples was performed. Tests were carried out to determine mechanical, hydraulic and physical properties on undamaged and damaged samples in order to characterize the effects of the damage mechanisms. From the results the main conclusions are:

- For GTX2 geotextile and for the GCR1 reinforcement geocomposite the characteristic opening size increased for all types of induced damage mechanisms, except for GCR1 after abrasion damage (2% reduction). These increases ranged from 25% to 45%. The permittivity of the geosynthetics did not increase accordingly, for most samples it decreased (between 1% and 30%). This opposite trend could be a consequence of the test setups;
- For the materials studied, the influence of the type of geosynthetic on the effects resulting from mechanical damage and abrasion damage were clear, namely in the peak tensile strength and stiffness for 2% of strain values. The structures of the GGRw woven geogrid and the GCR1 and GCR2 reinforcement geocomposites were more susceptible to induced damage compared with the other geosynthetics tested;
- As expected, the residual tensile strength of the geosynthetics damaged with a higher maximum loading is lower. However, the increased maximum loading used in mechanical damage tests from 500 kPa to 900 kPa (about 45%) did not cause proportional increases of strength losses;
- Generally, tensile strength losses after mechanical damage are lower than those caused by abrasion damage and the combined effect of mechanical and abrasion damage, indicating that susceptibility to abrasion damage can be more important to the tensile

response of these geosynthetics. The relevance of the abrasion is identical (except for the GTX1 geotextile), although with different degrees of severity;

- The strength losses for GTX1 and GTX2 geotextiles and for the GGRe extruded geogrid are much lower than for the other geosynthetics studied. The structure of the materials and how their constituents are affected by the mechanical and abrasion damage (observed visually) explains such differences;
- For the GGRw woven geogrid and the GCR1 and GCR2 reinforcement geocomposites, the effect of isolated abrasion seems to significantly condition their mechanical behaviour, namely their tensile strength;
- For most materials there is a positive synergy between mechanical damage and abrasion damage. If this trend is confirmed by tests under real conditions for applications of geosynthetics where abrasion is likely, the cumulative effects of these mechanisms should be considered instead of a superposition of their independent effects.

NOTATION

Basic SI units are given in parentheses.

d_{90}	particle size for which 90% of the mass fraction is smaller than the mass of measured particles (m)
D_{50}	average soil particle size (m)
$J_{sec\ 2\%}$	secant tensile stiffness modulus at 2% of strain (N/m)
mua_{nom}	nominal mass per unit area (kg/m^2)
$O_{90\ nom}$	nominal characteristic opening size (m)
O_{90}	characteristic opening size (m)
R_Y	Residual value of property Y (%)
t_{nom}	Nominal thickness (m)
T_{nom}	nominal peak tensile strength (N/m)
T_{max}	maximum tensile strength (N/m)
VI_{H50}	water flow velocity for a head loss of 50 mm (m/s)
Y_{dam}	mean value of property Y for the damaged sample
Y_{und}	mean value of property Y for the un damaged sample
ε_{nom}	nominal strain at break (dimensionless)
ε_f	strain at break (dimensionless)
ψ_{nom}	nominal permittivity (s^{-1})
ψ	permittivity (s^{-1})

PET	polyester
PP	Polypropylene
RF	Reduction factor
RF_{ID}	Reduction factor for installation damage

ACKNOWLEDGEMENTS

The authors would like to thank the financial support of FCT, Research Project PTDC/ECM/099087/2008 and COMPETE, Research Project FCOMP-01-0124-FEDER-009724.

REFERENCES

Allen TM and Bathurst RJ (1994) Characterization of geosynthetic load-strain behavior after installation damage. *Geosynthetics International* **1(2)**: 181-199.

Allen TM and Bathurst RJ (1996) Combined allowable strength reduction factor for geosynthetic creep and installation damage. *Geosynthetics International* **3(3)**: 407–439.

Bathurst RJ, Huang B and Allen TA (2011) Analysis of installation damage tests for LRFD calibration of reinforced soil structures. *Geotextiles and Geomembranes* **29**: 323-334.

Bräu G (1998) Experience with damage during installations in Germany – Field and laboratory testing. In *Proceedings of Seminar in Installation Damage in Geosynthetics*, ERA Technology, UK, pp. 2.1.1-2.1.15.

BSI (2008) EN ISO 10319 (2008). Geosynthetics. Wide-width tensile test. BSI, London, UK.

BSI (2007) EN ISO 10722 (2007). Geosynthetics. Index test procedure for the evaluation of mechanical damage under repeated loading - Damage caused by granular material. BSI, London, UK.

BSI (2010) EN ISO 11058 (2010). Geotextiles and geotextile-related products - Determination of water permeability characteristics normal to the plane, without load. BSI, London, UK.

BSI (2010) EN ISO 12956 (2010). Geotextiles and geotextile-related products. Determination of the characteristic opening size. BSI, London, UK.

BSI (1998) EN ISO 13427 (1998). Geotextiles and geotextile-related products. Abrasion damage simulation (sliding block test). BSI, London, UK.

BSI (2007) PD ISO/TR 20432 (2007). Guidelines to the determination of long-term strength of geosynthetics for soil reinforcement. BSI, London, UK.

BSI (1998) ENV ISO 10722-1 (1998). Geotextiles and geotextile-related products - Procedure for simulating damage during installation – Part 1: Installation in granular materials. BSI, London, UK.

Christopher BR and Elias V (1998) Evaluation of installation damage in geosynthetics: a US perspective. In *Proceedings of Seminar in Installation Damage in Geosynthetics*, ERA Technology, UK, pp. 1.2.1-1.2.12.

638 Hausmann MR, Ring GJ and Pitsis SE (1990) Abrasion of geotextiles in railway track
639 applications. In *Proceedings of the 4th International Conference on Geotextiles,*
640 *Geomembranes and Related Products*, pp. 193-196.
641 Huang C-C (2006) Laboratory simulation of installation damage of a geogrid. *Geosynthetics*
642 *International* **13(3)**: 120–132.
643 Huang C-C and Chiou S-L (2006) Investigation of installation damage of some geogrids
644 using laboratory tests. *Geosynthetics International* **13(1)**: 23–35.
645 Huang C-C and Liao C-C (2007) Abrasion damage of geogrids induced by turbid flow.
646 *Geotextiles and Geomembranes* **25**: 128–138.
647 Huang CC, Tzeng YS and Liao CJ (2007) Laboratory tests for simulating abrasion damage of
648 a woven geotextile. *Geotextiles and Geomembranes* **25**: 293–301.
649 Huang C-C and Wang Z-H (2007) Installation damage of geogrids: influence of load
650 intensity. *Geosynthetics International* **14(2)**: 65–75.
651 Hufenus R, Ruegger R, Flum D, and Sterba IJ (2005) Strength reduction factors due to
652 installation damage of reinforcing geosynthetics. *Geotextiles and Geomembranes* **23(5)**:
653 401-424.
654 Koerner RM (2005) Designing with geosynthetics. Prentice Hall, Upper Saddle River, New
655 Jersey, 5th edition.
656 Lim SY and McCartney JS (2013) Evaluation of effect of backfill particle size on installation
657 damage reduction factors for geogrids. *Geosynthetics International* **20(2)**: 62–72.
658 Lopes ML and Pinho-Lopes M (2010) Combined effect of damage during installation and
659 abrasion on the tensile behaviour of geotextiles. In *Proceedings of the 9th International*
660 *Conference on Geosynthetics*, Guarujá, Brasil, vol. 2, pp. 773-776.
661 Paula AM, Pinho-Lopes M and Lopes ML (2004) Damage during installation laboratory test.
662 Influence of the type of granular material. In *Proceedings of the 3rd European*
663 *Geosynthetics Conference*, Munich, Germany, pp. 603-606.
664 Pinho-Lopes M, Recker C, Lopes ML and Müller-Rochholz J (2002) Experimental analysis of
665 the combined effect of installation damage and creep of geosynthetics – new results. In
666 *Proceedings of the 7th International Conference on Geosynthetics*, Nice, France, vol. 4,
667 pp. 1539-1544.
668 Rosete AJ, Pinho-Lopes M and Lopes ML (2012) Effects of DDI in geocomposites'
669 mechanical and hydraulic behaviour: laboratory study. In *Proceedings of the 5th European*
670 *Geosynthetics Congress*. vol.1 Transport, pp. 155-160.

671 Shukla SK (2002) Geosynthetics and their applications. Chapter on “Fundamental of
672 geosynthetics”, Edited by S.K. Shukla, Thomas Telford, 430p.
673 Van Dine D, Raymond G and Williams SE (1982) An evaluation of abrasion tests for
674 geotextiles. In *Proceedings of the 2nd International Conference on Geotextiles*, Las Vegas,
675 USA, pp. 811-816.
676 Watn A and Chew SH (2002) Geosynthetic damage – from laboratory to field, Keynote
677 Lecture, In *Proceedings of the 7th International Conference on Geosynthetics*, Nice,
678 France, vol. 4, pp. 1203-1226.

TABLES

Table 1 - Nominal values for some properties of the geosynthetics studied.

Geosynthetic		T_{nom} (kN)	ε_{nom} (%)	ψ_{nom} (s^{-1})	$O_{90\ nom}$ (µm)	mua_{nom} (g/m^2)	t_{nom} (mm)	Grid spacing (mm)
GGRe	Extruded PP geogrid	40	11.0	-	-	-	1.4 to 5.8	33
GGRw	Woven PET geogrid	55	10.5	-	-	-	1.7	25
GTX1	Woven PP geotextile	50	65.0	0.50	<60	800	6.0	-
GTX2	Woven PP geotextile	55	105.0	0.16	75	1000	7.2	-
GCR1	Reinforcement geocomposite	55	10.0	1.40	95	321	2.1	-
GCR2	Reinforcement geocomposite	75	10.0	1.40	95	362	2.2	-

Table 2 – Test program implemented: wide-width tensile tests (EN ISO 10319).

Geosynthetic	Undamaged	Abrasion damage	Mechanical damage		Mechanical + Abrasion damage	
			500 kPa	900 kPa	500 kPa	900 kPa
GGRe	x	x	–	x	–	x
GGRw	x	x	x	x	x	x
GTX1	x	x	–	x	–	x
GTX2	x	x	x	x	x	x
GCR1	x	x	x	x	x	x
GCR2	x	x	x	x	x	x

Table 3 – Test program implemented: water permeability characteristics normal to the plane, without load (EN ISO 11058) and characteristic opening size (EN ISO 12956).

Geosynthetic	Undamaged	Abrasion damage	Mechanical damage (500 kPa)	Mechanical damage (500 kPa) + Abrasion
GTX2	x	x	x	x
GCR1	x	x	x	x

689 **Table 4 – Visual effects of mechanical and abrasion damage (in isolation and combined) on the**
690 **geosynthetics studied.**

Geosynthetic	Damage	Visual effects
GGRe	Abrasion	Reduction of the junction thickness (about 13%).
	Mechanical	No visible changes.
	Mechanical and Abrasion	Similar to abrasion.
GGRw	Abrasion	Detachment of the protective polymeric coating; disaggregation and cut of transversal ribs; splitting of longitudinal ribs.
	Mechanical	Some polyester fibre cutting; incrustation of fine particles.
	Mechanical and Abrasion	Similar to abrasion but a little more aggressive.
GTX1 GTX2	Abrasion	Partial disaggregation of superficial layer of geotextile without filament detachment of geotextile structure; preferential reorientation of filaments.
	Mechanical	Incrustation of fine particles resulting from corundum fragmentation.
	Mechanical and Abrasion	Superficial disaggregation; superficial filament cutting; filament reorientation originating a perpendicular accumulation of fibres in the machine direction of the geotextile.
GCR1 GCR2	Abrasion	Partial detachment and damage of PET yarns, i.e., the intertwined filaments that constitute the yarns split into two. Some perpendicular accumulation of fibres in the machine direction of the geocomposite occurs.
	Mechanical	Detachment and cuts of some of the PET yarns; incrustation of fines resulting from corundum fragmentation in the geotextile backing.
	Mechanical and Abrasion	Detachment and superficial disaggregation of the PET yarns; filament cutting and reorientation originating the perpendicular accumulation of fibres in the machine direction of the geocomposite.

691

692 **Table 5 – Mean permittivity (s^{-1}) and characteristic opening size (μm), with 95% confidence interval, for**
693 **undamaged and damaged samples of GTX2 and GCR1.**

	ψ (s^{-1})		O_{90} (μm)	
Sample	GTX2	GCR1	GTX2	GCR1
Undamaged	0.28 ± 0.05	1.27 ± 0.08	168.6 ± 31.9	207.8 ± 14.1
Abrasion	0.27 ± 0.05	1.28 ± 0.08	210.1 ± 24.9	204.4 ± 16.5
Mechanical (500kPa)	0.24 ± 0.04	1.27 ± 0.11	223.0 ± 20.5	301.2 ± 14.4
Mechanical (500kPa) + Abrasion	0.19 ± 0.02	1.07 ± 0.10	224.6 ± 70.7	223.2 ± 107.2

694

695

Table 6 – Mean values of tensile tests, with 95% confidence interval, for undamaged and damaged samples.

	Sample	T_{max} (kN/m)	ε_f (%)	$J_{sec\ 2\%}$ (kN/m)
GGRw	Undamaged	44.4 ± 1.1	8.1 ± 0.8	457.2 ± 45.6
	Abrasion	11.2 ± 3.2	8.9 ± 4.6	207.2 ± 74.1
	Mechanical (500kPa)	36.4 ± 3.3	7.4 ± 1.7	534.7 ± 68.3
	Mechanical (900kPa)	35.0 ± 2.8	7.4 ± 1.4	518.4 ± 53.6
	Mechanical (500kPa) + Abrasion	11.4 ± 2.2	5.6 ± 1.0	326.7 ± 65.7
	Mechanical (900kPa) + Abrasion	10.0 ± 2.6	6.9 ± 0.8	253.0 ± 48.1
GGRe	Undamaged	46.6 ± 1.2	12.2 ± 1.8	645.5 ± 321.0
	Abrasion	43.9 ± 2.3	10.9 ± 4.7	924.8 ± 452.8
	Mechanical (900kPa)	47.1 ± 0.3	10.8 ± 1.8	1014.9 ± 290.2
	Mechanical (900kPa) + Abrasion	44.7 ± 1.7	8.2 ± 4.5	1029.4 ± 321.4
GTX1	Undamaged	42.3 ± 3.4	89.3 ± 7.5	121.1 ± 36.5
	Abrasion	40.8 ± 8.3	113.2 ± 9.3	70.8 ± 21.7
	Mechanical (900kPa)	33.7 ± 5.1	84.6 ± 10.3	88.6 ± 53.8
	Mechanical (900kPa) + Abrasion	30.4 ± 2.2	96.9 ± 12.2	63.3 ± 20.7
GTX2	Undamaged	70.3 ± 3.7	107.4 ± 11.3	219.0 ± 52.6
	Abrasion	59.7 ± 4.8	102.6 ± 16.0	249.8 ± 120.4
	Mechanical (500kPa)	64.7 ± 3.3	107.7 ± 15.5	155.5 ± 22.9
	Mechanical (900kPa)	58.7 ± 4.2	79.2 ± 5.3	192.8 ± 35.5
	Mechanical (500kPa) + Abrasion	62.4 ± 2.9	97.7 ± 15.5	164.4 ± 25.0
	Mechanical (900kPa) + Abrasion	57.2 ± 3.6	93.0 ± 7.4	172.6 ± 71.9
GCR1	Undamaged	54.6 ± 2.3	10.6 ± 0.7	625.4 ± 124.4
	Abrasion	8.5 ± 2.0	5.1 ± 1.6	261.8 ± 61.3
	Mechanical (500kPa)	30.2 ± 2.8	13.0 ± 1.6	392.0 ± 90.2
	Mechanical (900kPa)	23.4 ± 4.3	10.1 ± 1.9	269.4 ± 85.3
	Mechanical (500kPa) + Abrasion	7.8 ± 0.8	7.9 ± 2.5	171.2 ± 48.1
	Mechanical (900kPa) + Abrasion	8.9 ± 1.3	8.5 ± 1.5	168.4 ± 27.7
GCR2	Undamaged	85.6 ± 6.8	14.2 ± 1.3	242.7 ± 209.4
	Abrasion	15.3 ± 2.8	15.2 ± 3.9	173.1 ± 57.9
	Mechanical (500kPa)	52.2 ± 1.1	12.3 ± 0.8	473.6 ± 105.7
	Mechanical (900kPa)	43.1 ± 2.4	16.4 ± 6.5	641.7 ± 148.6
	Mechanical (500kPa) + Abrasion	14.2 ± 1.7	7.5 ± 1.6	288.9 ± 207.3
	Mechanical (900kPa) + Abrasion	14.2 ± 0.5	9.1 ± 2.5	250.5 ± 109.1

Table 7 – Reduction factors for the permittivity obtained from the mean values of the test results.

Damage	GTX2	GCR1
Abrasion	1.02	1.00
Mechanical (500kPa)	1.15	1.00
Mechanical (500kPa) + Abrasion	1.43	1.18
Mechanical (500kPa) x Abrasion (traditional)	1.15	1.00

Table 8– Reduction factors for the characteristic opening size obtained from the mean values of the test results.

Damage	GTX2	GCR1
Abrasion	0.80	1.02
Mechanical (500kPa)	0.76	0.69
Mechanical (500kPa) + Abrasion	0.75	0.93
Mechanical (500kPa) x Abrasion (traditional)	0.61	0.70

Table 9 – Reduction factors for the tensile strength obtained from the results and using the traditional approach.

Damage	GGRw	GGRe	GTX1	GTX2	GCR1	GCR2
Abrasion	3.98	1.1	1.04	1.18	6.40	5.59
Mechanical (500kPa)	1.22	-	-	1.09	1.81	1.64
Mechanical (900kPa)	1.27	0.99	1.26	1.20	2.34	1.99
Mechanical (500kPa) + Abrasion	3.90	-	-	1.13	6.98	6.02
Mechanical (900kPa) + Abrasion	4.45	1.04	1.39	1.23	6.14	6.04
Mechanical (500kPa) x Abrasion (traditional)	4.85	-	-	1.28	11.57	9.16
Mechanical (900kPa) x Abrasion (traditional)	5.04	1.05	1.30	1.41	14.97	11.11

FIGURES

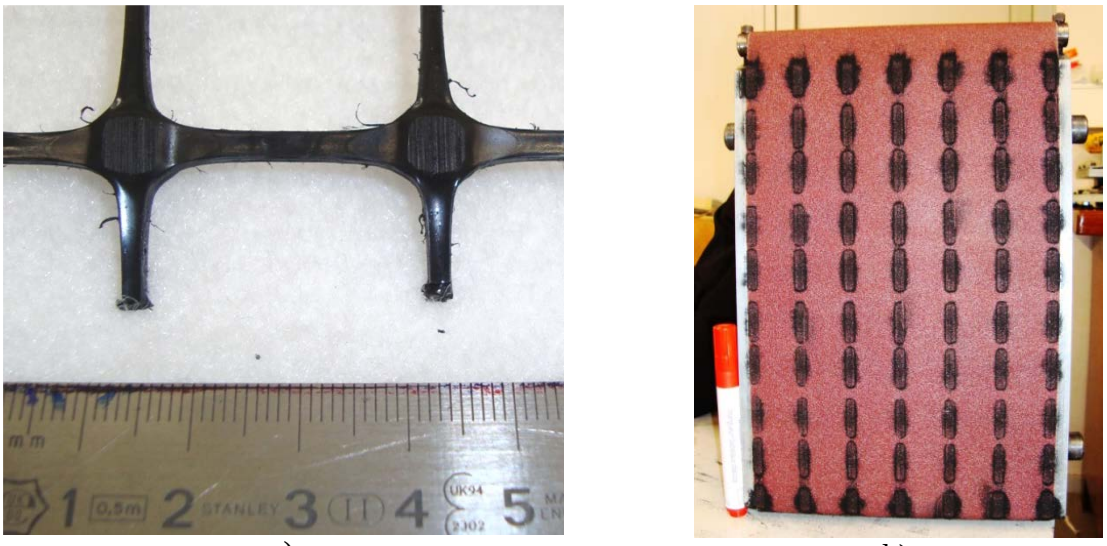

a) b)

Figure 1 – Visual effects of abrasion damage tests on GGRe (a) and on the abrasion film (b).

713

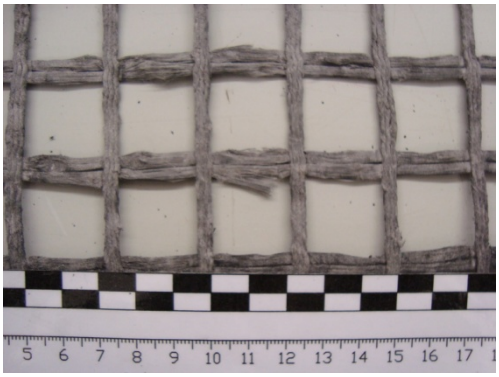

a)

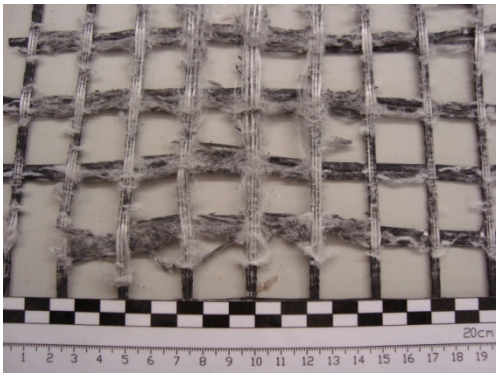

b)

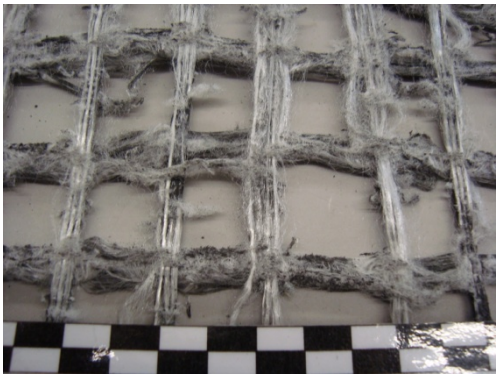

c)

714 **Figure 2 – Visual effects on GGRw after tests: a) mechanical damage with 900 kPa; b) abrasion; c)**
715 **mechanical damage with 900 kPa followed by abrasion.**

716

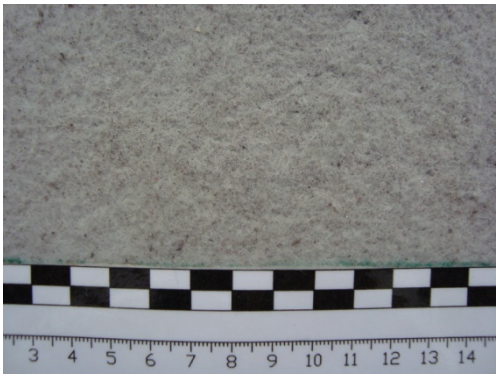

a)

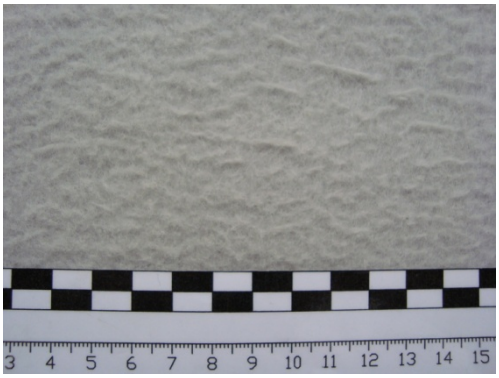

b)

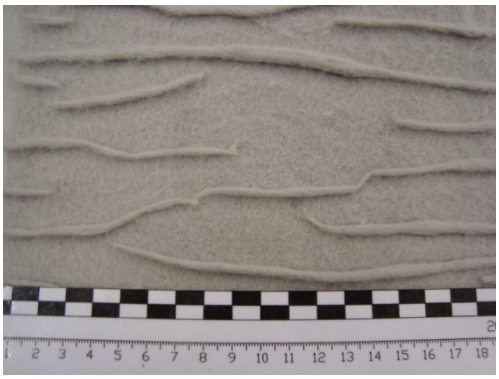

c)

Figure 3 – Visual effects on GTX2 after tests: a) mechanical damage with 900 kPa; b) abrasion; b) mechanical damage with 900 kPa followed by abrasion.

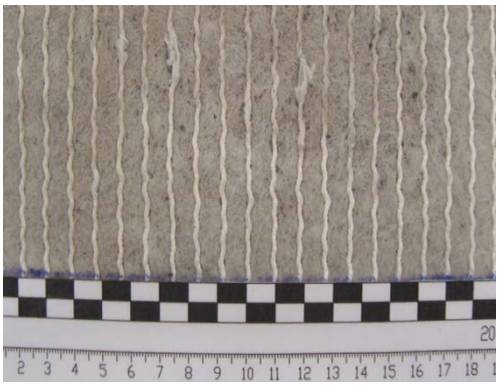

a)

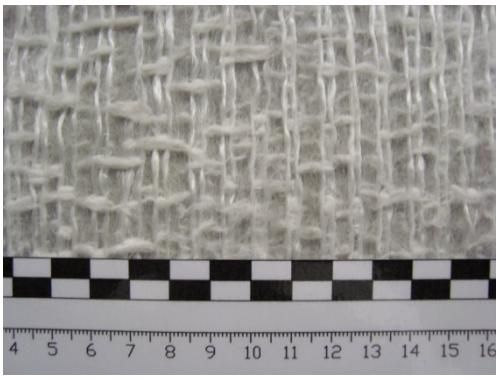

b)

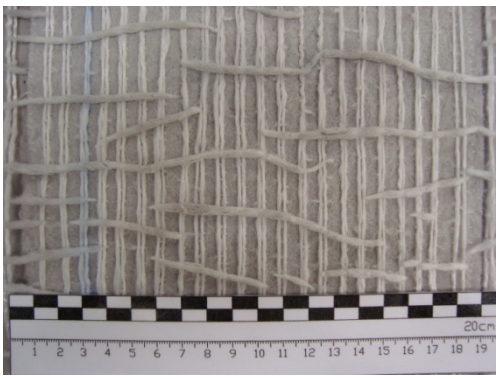

c)

Figure 4 – Visual effects on GCR2 after tests: a) mechanical damage with 900 kPa; b) abrasion; c) mechanical damaged with 900 kPa followed by abrasion.

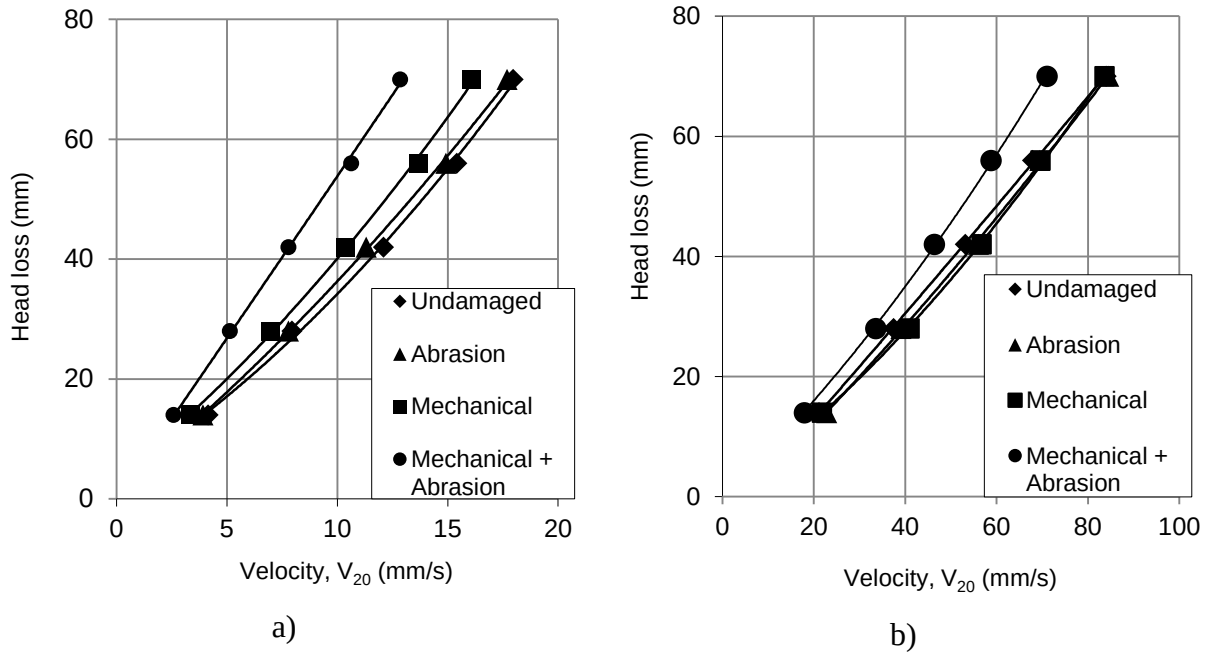

724 **Figure 5 – Water flow velocity at a temperature of 20ºC (mm/s) for different head losses (mm) after**
725 **laboratory tests (specimens nearest to the mean of the corresponding sample): a) GTX2; b) GCR1.**
726
727

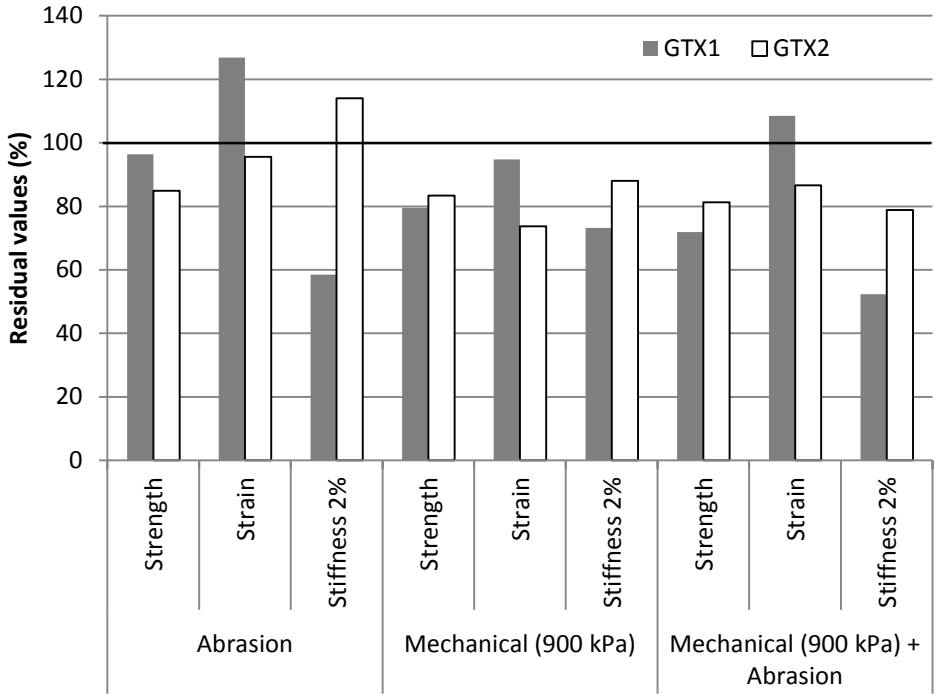

728
729 **Figure 6 – Residual values of tensile strength, peak strain, and stiffness for 2% strain (%) of GTX1 and**
730 **GTX2 after laboratory damage tests.**
731

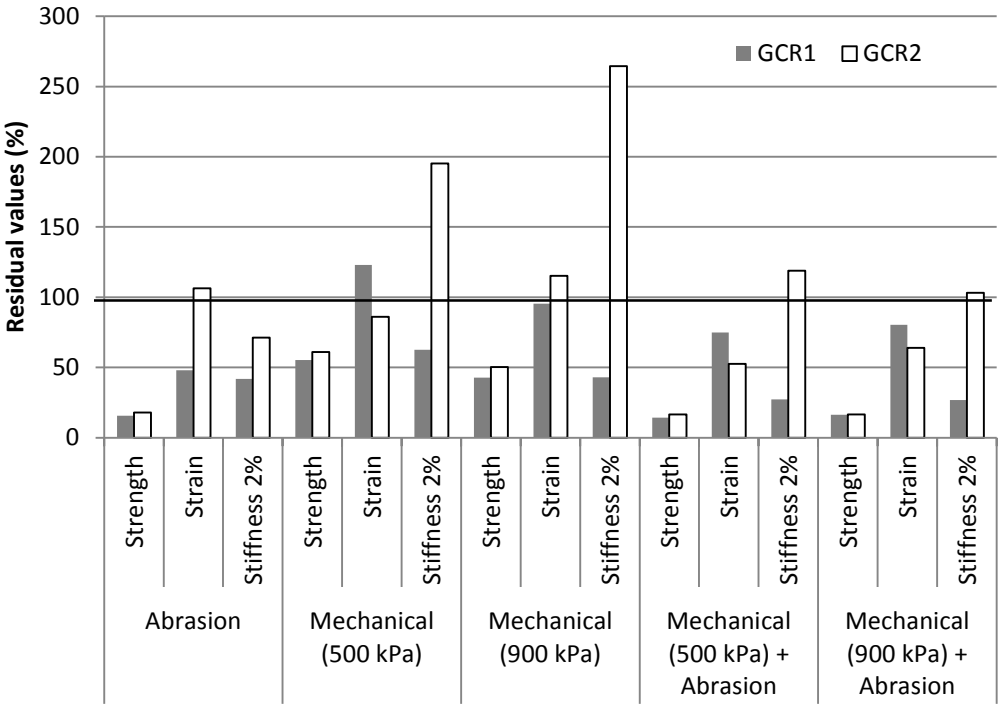

732

733 **Figure 7 – Residual values of tensile strength, peak strain and stiffness for 2% strain (%) of GCR1 and**
734 **GCR2 after laboratory damage tests.**

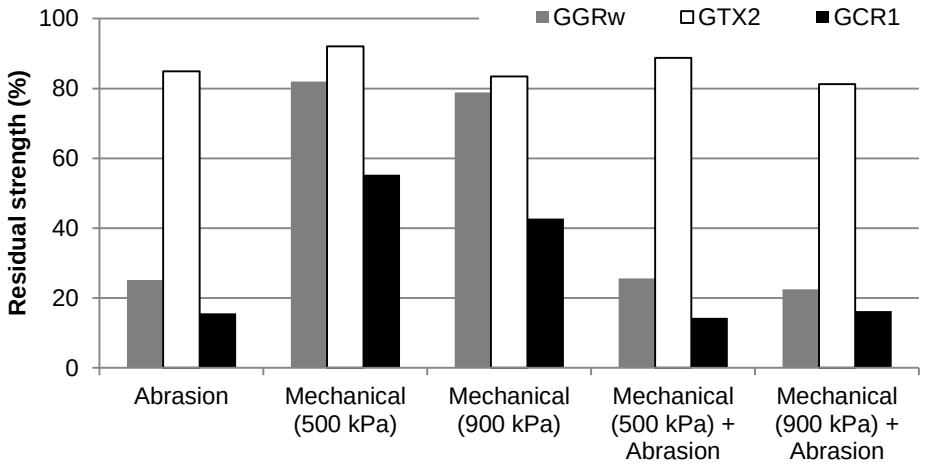

735

736 **Figure 8 – Residual tensile strength (%) of GGRw, GTX2 and GCR1 (different structures and nominal**
737 **strength of 55 kN/m) after laboratory damage tests.**

738

739

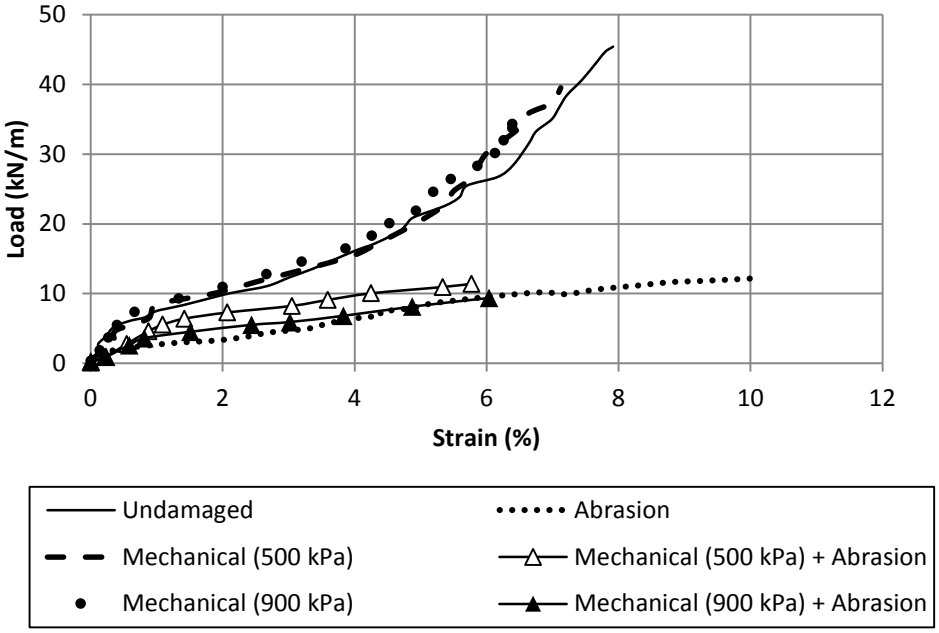

740

741 **Figure 9 – Representative load-strain curves of GGRw after the laboratory damage tests.**

742

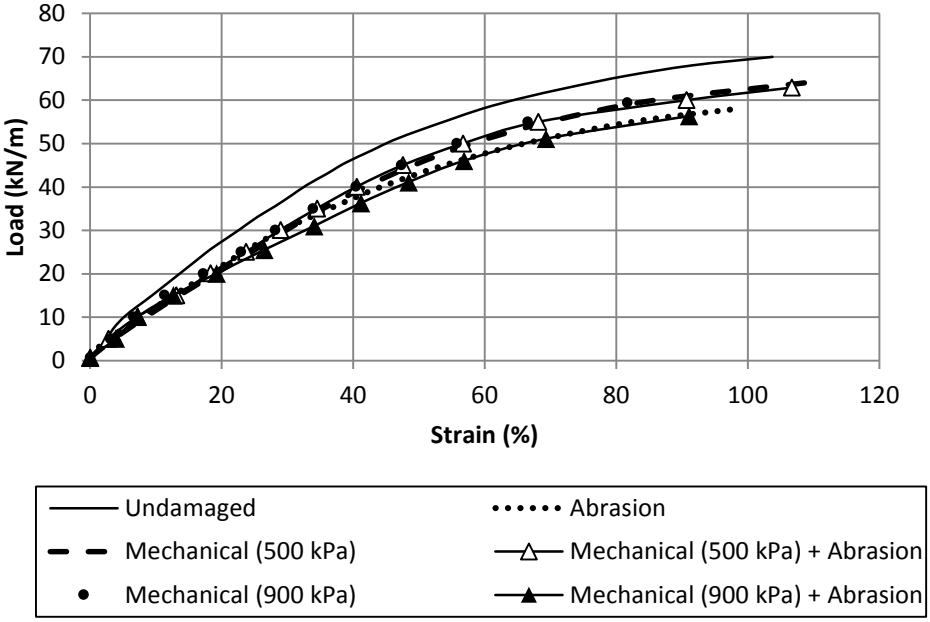

743

744 **Figure 10 – Representative load-strain curves of GTX2 after the laboratory damage tests.**

745

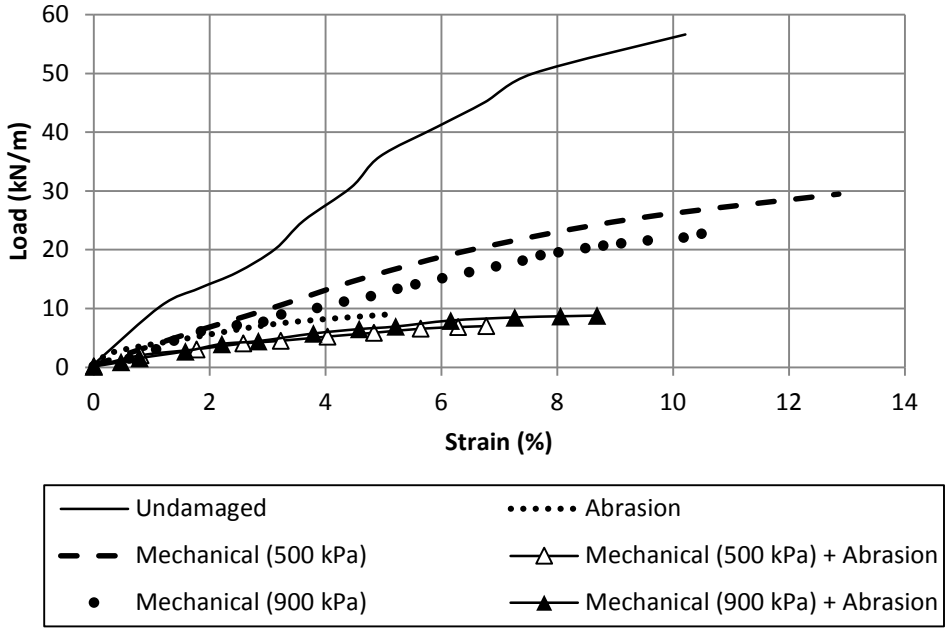

746

747 **Figure 11 – Representative load-strain curves of GCR1 after the laboratory damage tests.**

748

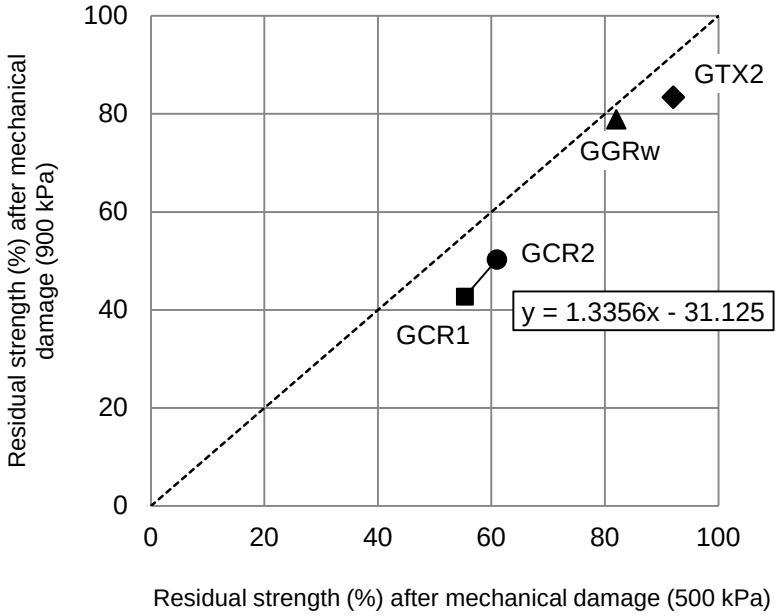

749

750 **Figure 12 –Residual tensile strength after mechanical damage in the laboratory with a maximum load of**
751 **500 kPa vs 900 kPa.**

752

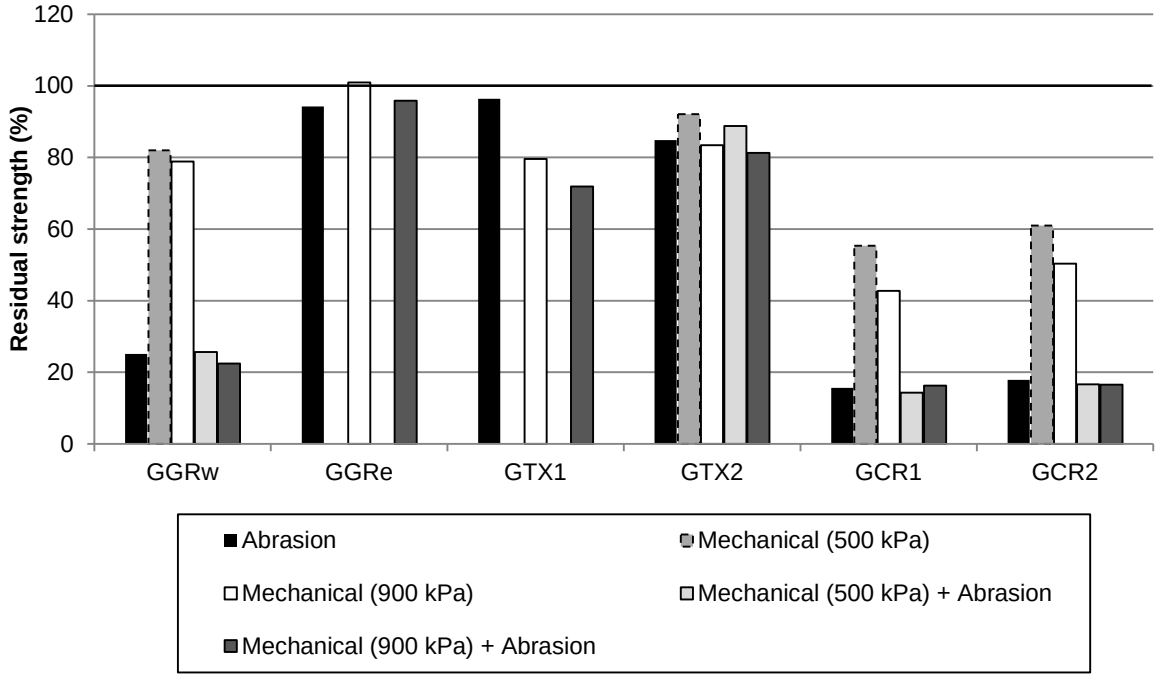

753

754 **Figure 13 – Residual tensile strength (%) of the geosynthetics studied after laboratory tests of mechanical**
755 **damage, abrasion damage and their combination.**

756

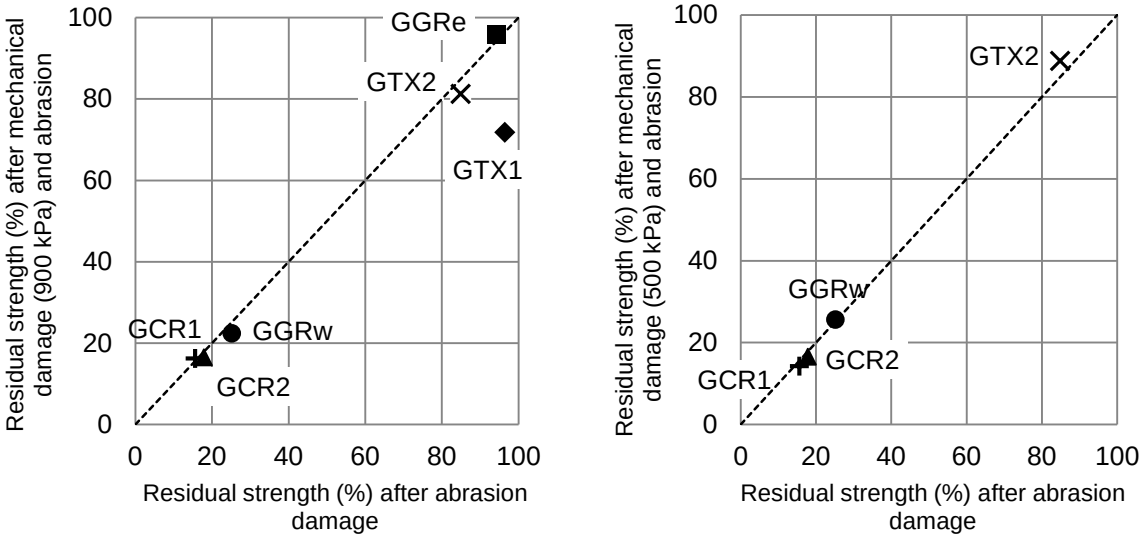

a) b)

757 **Figure 14 –Residual tensile strengths: a) abrasion vs mechanical damage with 900 kPa followed by**
758 **abrasion; abrasion vs mechanical damage with 500 kPa followed by abrasion.**

759